PAIN

The mechanosensitive ion channel Piezo2 mediates sensitivity to mechanical pain in mice

Swetha E. Murthy[1], Meaghan C. Loud[1], Ihab Daou[1], Kara L. Marshall[1], Frederick Schwaller[2], Johannes Kühnemund[2], Allain G. Francisco[1], William T. Keenan[1], Adrienne E. Dubin[1], Gary R. Lewin[2,3], Ardem Patapoutian[1]*

The brush of a feather and a pinprick are perceived as distinct sensations because they are detected by discrete cutaneous sensory neurons. Inflammation or nerve injury can disrupt this sensory coding and result in maladaptive pain states, including mechanical allodynia, the development of pain in response to innocuous touch. However, the molecular mechanisms underlying the alteration of mechanical sensitization are poorly understood. In mice and humans, loss of mechanically activated PIEZO2 channels results in the inability to sense discriminative touch. However, the role of Piezo2 in acute and sensitized mechanical pain is not well defined. Here, we showed that optogenetic activation of *Piezo2*-expressing sensory neurons induced nociception in mice. Mice lacking *Piezo2* in caudal sensory neurons had impaired nocifensive responses to mechanical stimuli. Consistently, ex vivo recordings in skin-nerve preparations from these mice showed diminished Aδ-nociceptor and C-fiber firing in response to mechanical stimulation. Punctate and dynamic allodynia in response to capsaicin-induced inflammation and spared nerve injury was absent in Piezo2-deficient mice. These results indicate that Piezo2 mediates inflammation- and nerve injury–induced sensitized mechanical pain, and suggest that targeting PIEZO2 might be an effective strategy for treating mechanical allodynia.

INTRODUCTION

In humans, inflammation or nerve injury can cause abnormal sensory processing, which results in exaggerated responses to innocuous or noxious mechanical stimuli (*1*, *2*). Mechanical allodynia is one such sensitized mechanical pain state and is thought to be caused either by sensitization of peripheral sensory neurons or by amplification of the signal at the spinal cord level (*1*). Mechanical allodynia is one of the leading symptoms in clinical pain and manifests in multiple forms: dynamic allodynia evoked by something as gentle as a brush stroke, static allodynia evoked by pressure, and punctate allodynia elicited by pinch-like stimuli such as von Frey filaments (*3*–*6*). Mouse pain models that mimic symptoms of punctate and dynamic allodynia have been used to study these abnormal pain pathways (*7*–*9*). However, very little is known about the molecular mechanisms that mediate sensitized mechanical pain at the periphery.

Innocuous and noxious mechanical stimuli are detected by sensory neurons called low-threshold mechanoreceptors (LTMRs) and nociceptors, respectively, primarily by activating mechanically activated ion channels (*10*–*12*). In mice and humans, PIEZO2 is expressed by a subpopulation of sensory neurons and is the principal mechanically activated nonselective cation channel that detects mechanical forces relevant for touch sensation, proprioception (the ability to sense body position), and respiration (*13*–*17*). In mice, two different Piezo2 knockout strategies have been used to determine their contribution to the somatosensory system. To elucidate the role of Piezo2 in tactile sensation, a tamoxifen-inducible AdvillinCreERT2 mouse line has been used to delete *Piezo2* in all adult sensory neurons (*14*). While discriminative touch was severely affected in AdvillinCre;Piezo2^{cKO} mice, response to noxious mechanical stimuli and inflammatory pain were normal. Piezo2's role in proprioception was assessed with the HoxB8Cre mouse line, which generates a constitutive *Piezo2* knockout that is anatomically restricted to caudal sensory neurons (*15*, *18*). Although acute and sensitized mechanical pain responses were not tested in these mice, the proprioceptive deficits in HoxB8Cre;Piezo2^{KO} were stronger than those observed in AdvillinCre;Piezo2^{cKO}. Therefore, somatosensory tests in *Piezo2*-deficient mice and in PIEZO2 loss-of-function humans have suggested that PIEZO2 is not required for mechanical nociception (*14*, *17*). However, because *Piezo2* mRNA is present in nociceptors (*13*, *19*, *20*), we reevaluated the role of Piezo2 in pain and, importantly, we asked whether Piezo2 is required for mechanical allodynia.

RESULTS

Activation of *Piezo2*-expressing neurons evokes painful behavior in mice

To elucidate the role of Piezo2 in pain, we first tested whether optogenetic activation of *Piezo2*-expressing sensory afferents can generate nocifensive responses in behaving mice. We used two strategies to express the light-activated ion channel, channelrhodopsin-2 (ChR2), in *Piezo2*-expressing neurons: (i) ChR2 was constitutively expressed in cells from *Piezo2* lineage by crossing Piezo2-GFP-IRES-Cre mice (*21*) to Ai32 mice ("constitutive Piezo2-ChR2$^+$ mice"; Fig. 1A and fig. S1A) (*22*) and (ii) ChR2 was postnatally expressed in *Piezo2* lineage cells by intraperitoneal injection of adeno-associated virus 8 (AAV8) carrying a Cre-dependent ChR2-tdTomato construct in postnatal day P0 to P2 Piezo2-GFP-IRES-Cre pups ("postnatal Piezo2-ChR2$^+$ mice"; Fig. 1A and fig. S1B). We observed that 28.55 ± 1.92% of dorsal root ganglion (DRG) neurons

[1]Howard Hughes Medical Institute, Department of Neuroscience, The Scripps Research Institute, La Jolla, CA 92037, USA. [2]Department of Neuroscience, Max Delbrück Center for Molecular Medicine, Robert-Rössle Straße 10, Berlin 13125, Germany. [3]Excellence Cluster Neurocure, Charité Universitätsmedizin, Berlin 13125, Germany.
*Corresponding author. Email: ardem@scripps.edu

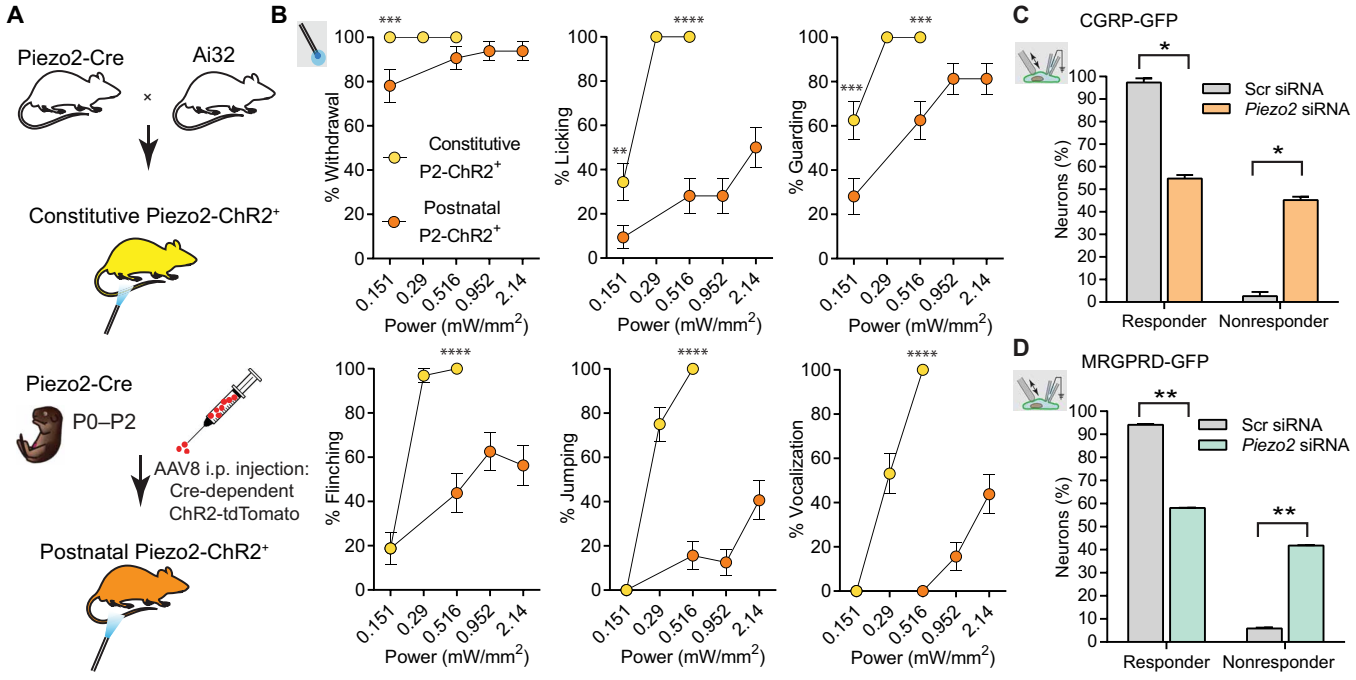

Fig. 1. Activation of *Piezo2*-expressing neurons evoke nocifensive behavior. (**A**) Schematic describing genetic strategy for generating constitutive and postnatal Piezo2-ChR2–positive mice (P2-ChR2$^+$). i.p., intraperitoneal. (**B**) Percent behavioral response (paw withdrawal, paw licking, paw guarding, flinching, jumping, and vocalization) in constitutive Piezo2-ChR2$^+$ ($n = 8$) and postnatal Piezo2-ChR2$^+$ ($n = 12$) mice evoked by blue light (462 nm) stimulation (2 Hz, 100-ms pulses) of the plantar surface of the hindpaws [% withdrawal: ***$P = 0.0006$; % licking: **$P = 0.0092$ and ****$P < 0.0001$; % guarding: ***$P = 0.0009$ (0.151 mW/mm^2) and ***$P = 0.0002$ (0.516 mW/mm^2); % flinching: ****$P < 0.0001$; % jumping: ****$P < 0.0001$; % vocalization: ****$P < 0.0001$; two-way analysis of variance (ANOVA) Sidak's multiple comparison test]. (**C** and **D**) Bar graphs representing frequency distribution of DRG neurons characterized by the presence (responders) or absence (nonresponders) of mechanically activated currents; DRG neurons cultured from CGRP-GFP (C) and MRGPRD-GFP (D) mice. Mechanically activated currents were recorded from green fluorescent protein (GFP)–positive neurons transfected with scrambled siRNA (CGRP, $n = 32$; MRGPRD, $n = 50$) or *Piezo2* siRNA (CGRP, $n = 33$; MRGPRD, $n = 43$). Data from two to three independent experiments [*$P = 0.006$, **$P = 0.003$ (responder), and **$P = 0.002$ (nonresponder), nonparametric t test].

were virally transduced (fig. S1C). In constitutive and postnatal Piezo2-ChR2$^+$ mice, photostimulation on plantar surface of the hindpaw with blue light [but not yellow light, a wavelength that does not activate ChR2 (*23*)] evoked paw withdrawal and various other nocifensive behaviors such as paw licking, guarding, flinching, jumping, and vocalization (Fig. 1B). Wild-type mice, on the other hand, did not respond to blue light photostimulation of the hindpaw (fig. S1D). Postnatal Piezo2-ChR2$^+$ mice exhibited weaker responses compared to those from constitutive Piezo2-ChR2$^+$ mice. These results indicate that activating *Piezo2*-positive somatosensory afferents is sufficient to induce nociception, consistent with expression of *Piezo2* in nociceptors.

Next, we examined whether functional Piezo2 protein is present in genetically marked nociceptor populations of mouse DRG neurons. Specifically, we tested whether mechanically activated currents in two major nociceptor subtypes, calcitonin gene–related peptide (CGRP) receptor–expressing peptidergic neurons (*24*) and Mas-related G protein coupled receptor subtype D (MRGPRD)–expressing nonpeptidergic neurons (*25*), are dependent on Piezo2. Knocking down *Piezo2* by transfecting cultured DRG neurons with *Piezo2* small interfering RNA (siRNA) revealed an increase in mechanically insensitive neurons in both nociceptor subtypes (Fig. 1, C and D, and fig. S2, A and B). This suggests that Piezo2 can mediate mechanically activated currents in nociceptors.

Mechanical nociception in *Piezo2*-deficient mice is partially impaired

We next addressed whether *Piezo2* is required for mechanical nociception. We first tested the efficiency of *Piezo2* ablation in the previously described *Piezo2* knockout mouse lines, AdvillinCre;Piezo2^{cKO} (Piezo2^{iAdv}) and HoxB8Cre;Piezo2^{KO} (Piezo2^{HoxB8}), to determine whether constitutive Cre expression is a more efficient recombinase system compared to inducible Cre. We compared *Piezo2* mRNA levels in the DRG from wild-type (Piezo2^{WT}), Piezo2^{iAdv}, and Piezo2^{HoxB8} mice and showed that HoxB8Cre induces a more complete ablation of *Piezo2* (Fig. 2A). We also directly compared cutaneous mechanosensitivity of Piezo2^{HoxB8} and Piezo2^{iAdv} mice by assessing paw withdrawal responses elicited by a range of mechanical forces using von Frey filaments. Unlike Piezo2^{iAdv} mice, which have impaired responses only at low filament strengths, Piezo2^{HoxB8} mice showed diminished responses at low and high mechanical forces (Fig. 2B).

To verify that the difference in von Frey force responses between the two mouse lines was not due to the severe proprioceptive deficit in Piezo2^{HoxB8} mice, we tested their ability to respond to heat. The threshold for temperature response was indistinguishable between wild-type and Piezo2^{HoxB8} mice (Fig. 2C), indicating that these mice have sufficient motor coordination to react to a noxious stimulus on their hindpaw. In addition, Piezo2^{HoxB8} mice have a normal

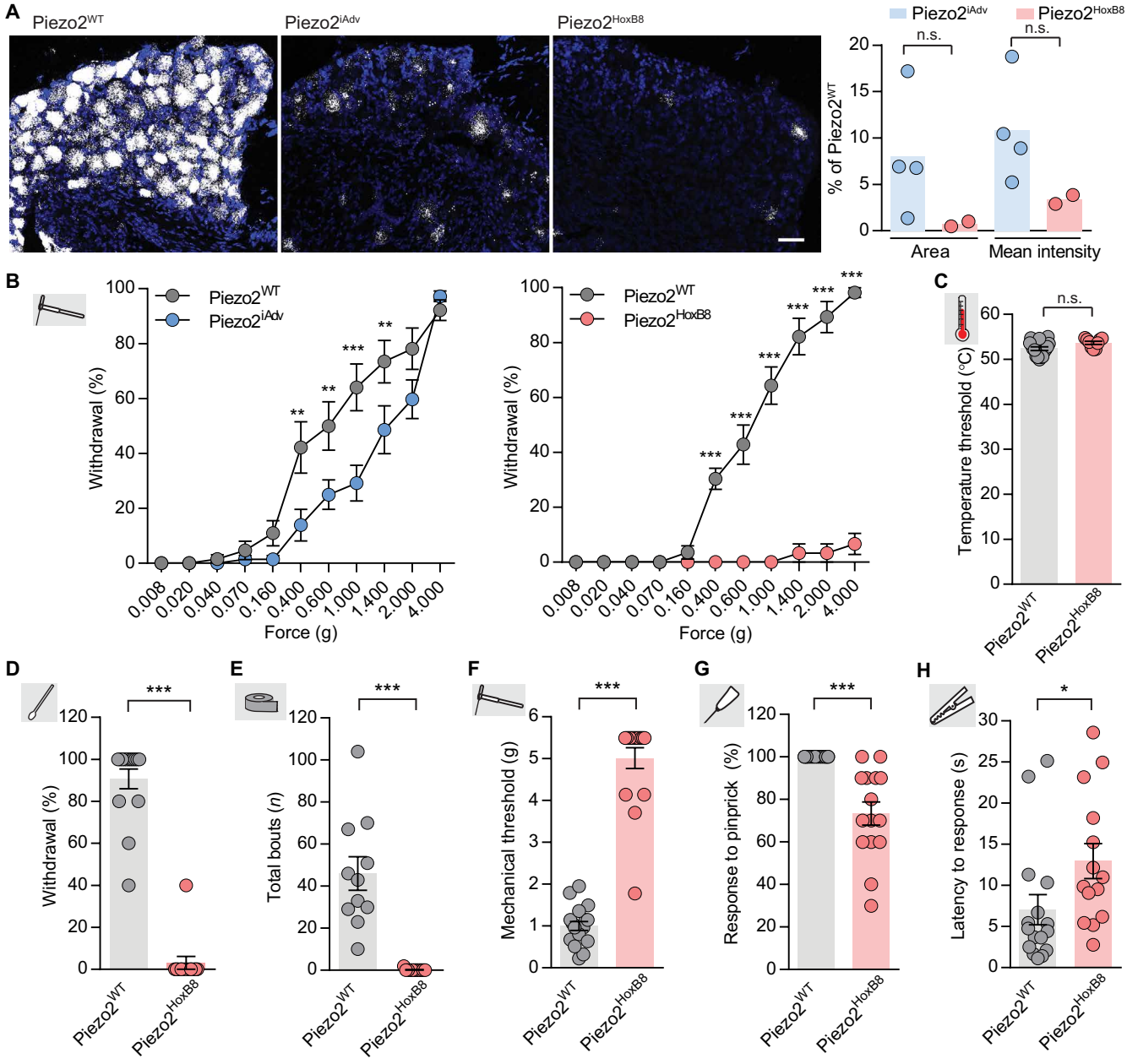

Fig. 2. Mechanical nociception is partially Piezo2 dependent. (**A**) Representative images of *Piezo2* in situ hybridization in lumbar DRG sections from wild-type (Piezo2^{WT}; $n = 3$), AdvillinCreERT2 (Piezo2^{iAdv}; $n = 4$), and HoxB8Cre (Piezo2^{HoxB8}; $n = 2$) mice. White, *Piezo2* transcript; blue, 4′,6-diamidino-2-phenylindole (DAPI). Scale bar, 25 μm. Right: Quantification of *Piezo2* transcript labeling area and mean intensity. Each dot represents mean values from one mouse. Bars represent population mean. (**B**) Percent paw withdrawal (four trials) in response to von Frey filament at different forces in Piezo2^{iAdv} mice [left; Piezo2^{WT}, $n = 16$; Piezo2^{iAdv}, $n = 18$; $^{**}P = 0.002$ (0.4*g*), $^{**}P = 0.008$ (0.6*g*), $^{***}P < 0.0001$ (1.0*g*), and $^{**}P = 0.008$ (1.4*g*), one-way ANOVA with Holm-Sidak's multiple comparison test] and Piezo2^{HoxB8} mice (right; Piezo2^{WT}, $n = 14$; Piezo2^{HoxB8}, $n = 15$) (data at each force are means ± SEM; one-way ANOVA with Holm-Sidak's multiple comparison test, $^{***}P < 0.0001$). (**C**) Thermal paw withdrawal threshold measured with a thermal probe in Piezo2^{WT} ($n = 16$) and Piezo2^{HoxB8} ($n = 9$) mice. (**D**) Percent response (five trials) to cotton swab stroke on the hindpaw in Piezo2^{WT} ($n = 15$) and Piezo2^{HoxB8} ($n = 13$) mice. (**E**) Number of bouts observed in response to an adhesive tape applied to the lower back of Piezo2^{WT} ($n = 11$) and Piezo2^{HoxB8} ($n = 11$) mice. (**F**) Mechanical threshold measured in the range of 0.04*g* to 6*g* in Piezo2^{WT} ($n = 18$) and Piezo2^{HoxB8} ($n = 17$) mice. (**G**) Percent response (10 trials) to pinprick on hindpaw in Piezo2^{WT} ($n = 16$) and Piezo2^{HoxB8} ($n = 15$) mice. (**H**) Latency to response when an alligator clip (500*g*) is placed on the base of the tail in Piezo2^{WT} ($n = 16$) and Piezo2^{HoxB8} ($n = 14$) mice. Data for all experiments were collected from at least three separate cohorts of both male and female littermate wild-type mice. (A and C to H) Bars represent means ± SEM; $^{*}P = 0.011$ and $^{***}P < 0.0001$, n.s., not significant, Mann-Whitney nonparametric analysis.

blink reflex to mechanical stimulation of the eye, whose sensory innervation does not express HoxB8 (fig. S3). The more complete loss of *Piezo2* mRNA and the stronger von Frey phenotype validated Piezo2^{HoxB8} mice as more efficient *Piezo2* knockouts than Piezo2^{iAdv} mice. Given these results, in the subsequent experiments, we examined the contribution of Piezo2 in nociception and sensitized mechanical pain using the Piezo2^{HoxB8} mice.

As expected, Piezo2^{HoxB8} mice had strong deficits in response to innocuous mechanical stimuli, such as from stroking the hindpaw with a cotton swab (Fig. 2D and fig. S4A) and applying tape on the back (Fig. 2E and fig. S4B) (*14*). Cutaneous mechanosensitivity in mice can also be quantified as the magnitude of force required to evoke paw withdrawal to a stimulus (*26*). Piezo2^{HoxB8} mice had fivefold higher withdrawal threshold to mechanical stimuli to the hindpaw compared to wild-type mice (Fig. 2F and fig. S4C). These results suggest that the ability to sense mechanical stimuli at higher forces is impaired in *Piezo2*-deficient mice. Furthermore, the behavioral response to purely noxious mechanical stimuli such as pinprick (Fig. 2G and fig. S4D) or blunt pressure application with an alligator clip (Fig. 2H and fig. S4E) was also compromised in Piezo2^{HoxB8} mice; however, the deficit is less severe than what was observed in response to innocuous mechanical stimuli (Fig. 2, D to F).

Piezo2^{HoxB8} mice exhibit reduced nociceptor firing

The sensation of fast punctate pain inflicted by a pinprick is carried by Aδ-nociceptors (*27*). Detection of blunt pressure, on the other hand, is transduced by C-fiber nociceptors in mice (*28*, *29*). However, there is some debate over the nociceptor subtypes that respond to different noxious mechanical stimuli between rodents and humans (*30*, *31*). Regardless, we hypothesized that the diminished response to noxious mechanical stimuli in Piezo2^{HoxB8} mice could be due to impaired mechanosensitivity of Aδ-nociceptors and C-fibers. To test this, we used an ex vivo saphenous skin-nerve preparation to electrophysiologically record Aβ-, Aδ-, and C-fiber responses to mechanical stimulation from Piezo2^{HoxB8} and wild-type mice (Fig. 3A). Similar to what was observed in Piezo2^{iAdv} mice, the number of mechanically insensitive Aβ-fibers (which are almost exclusively LTMRs) was higher in Piezo2^{HoxB8} mice (Fig. 3B) (*14*). In addition, we observed deficiency of Aδ- and C-fiber mechanosensitivity in Piezo2^{HoxB8} mice. Specifically, although the number of Aδ- and C-fibers with mechanical responses was not affected, the threshold for response in Aδ-fibers was higher (Fig. 3B and fig. S5A). Moreover, at the highest mechanical force used (400 mN), both Aδ- and C-fibers in Piezo2^{HoxB8} had reduced activity (measured as spike frequency) during the first 2 to 3 s of the applied stimulus (Fig. 3, C to F). This suggests that loss of *Piezo2* impairs the firing frequency of Aδ-nociceptors and C-fibers that transduce the sensation of fast punctate and blunt pain. Therefore, the attenuated nociceptor firing and the impaired behavioral responses to noxious mechanical stimuli in Piezo2^{HoxB8} mice demonstrate that Piezo2 does contribute to noxious mechanosensation in mice.

Piezo2 mediates mechanical allodynia

We had previously reported that bradykinin and complete Freund's adjuvant–induced inflammatory mechanical pain were not affected in Piezo2^{iAdv} mice (*14*). Paradoxically, a partial (25 to 50%) knockdown of *Piezo2* mRNA in mice was reported to cause a short-term reduction in chronic constriction injury and chemotherapy-induced mechanical hypersensitivity (*32*, *33*). Here, we revisited the contribution

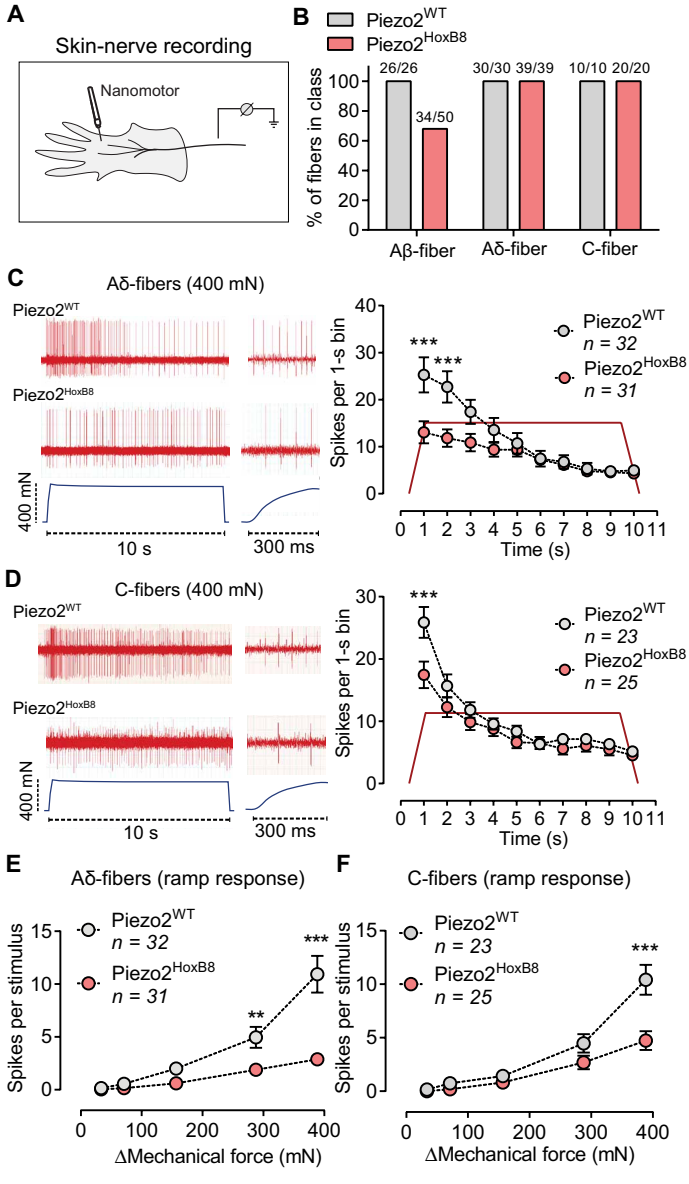

Fig. 3. Mechanical stimuli–induced nociceptor firing is impaired in Piezo2^{HoxB8} mice. (**A**) Schematic of ex vivo saphenous skin-nerve preparation. (**B**) Percentage of mechanically sensitive Aβ-, Aδ-, and C-fibers in wild-type and Piezo2^{HoxB8} mice. (**C**) Left: Representative example of Aδ-fiber firing activity during 400-mN mechanical stimulation in Piezo2^{WT} and Piezo2^{HoxB8} mice. Responses to the ramp phase of the stimulus are enlarged and shown on the right. Right: Mean Aδ-fiber firing activity during the 400-mN stimulation in Piezo2^{WT} and Piezo2^{HoxB8} mice (repeated-measures two-way ANOVA with Bonferroni post hoc analysis, ***$P < 0.001$). (**D**) Left: Representative example of C-fiber firing activity during 400-mN mechanical stimulation in Piezo2^{WT} and Piezo2^{HoxB8} mice. Right: Mean C-fiber firing activity during the 400-mN stimulation in Piezo2^{WT} and Piezo2^{HoxB8} mice (***$P < 0.001$, repeated-measures two-way ANOVA with Bonferroni post hoc analysis). (**E** and **F**) Spike activity during ramp phase of high-force mechanical stimulation in Piezo2^{WT} and Piezo2^{HoxB8} Aδ-fibers (E) (repeated-measures two-way ANOVA with Bonferroni post hoc analysis, **$P < 0.01$ and ***$P < 0.001$) and in C-fibers (F) (repeated-measures two-way ANOVA with Bonferroni post hoc analysis, ***$P < 0.001$). Data are represented as means ± SEM. (B to F) *n* values indicate number of fibers recorded from. Data were collected across multiple mice for each genotype. Piezo2^{WT}, *n* = 10 mice; Piezo2^{HoxB8}, *n* = 8 mice.

of Piezo2 to inflammatory and nerve injury–induced mechanical allodynia in Piezo2^{HoxB8} mice.

We first tested whether mechanical allodynia in an acute inflammation model was Piezo2 mediated. Cutaneous inflammation can be induced in mice by different methods, including administration of compounds that activate nociceptors (*34*). For instance, intradermal injection of capsaicin activates the nociceptor-specific transient receptor potential cation channel V1 and causes sensitization to peripheral stimuli (*35*). Because capsaicin-induced transient inflammation is commonly used as an experimental pain model in humans, we tested Piezo2's contribution to capsaicin-induced punctate and dynamic mechanical allodynia. Capsaicin injection in wild-type and Piezo2^{HoxB8} mice induced inflammation and thermal hyperalgesia to a comparable extent (fig. S6, A and B). In wild-type mice, capsaicin injection lowered the mechanical threshold from von Frey filament stimulation and evoked nocifensive behavior in response to a brush stroke on the plantar surface of the hindpaw (Fig. 4, A and B, and fig. S7, A to C). Capsaicin injection in Piezo2^{HoxB8} mice neither reduced the mechanical threshold nor induced brush-evoked pain (Fig. 4, A and B, and fig. S7, A to C). In addition, capsaicin injection in Piezo2^{iAdv} mice lowered the mechanical threshold, but to a lesser extent than in wild-type mice, suggesting that knocking down *Piezo2* in adult mice also affected capsaicin-induced mechanical allodynia (fig. S8). These results together indicate that Piezo2 is a key ion channel that mediates capsaicin-induced mechanical allodynia in mice.

We next tested the role of Piezo2 in mechanical allodynia in the spared nerve injury (SNI) model. As expected, wild-type mice exhibited reduced mechanical threshold up to 21 days after injury; the mechanical threshold in Piezo2^{HoxB8} mice did not change throughout the experiment (Fig. 4C and fig. S9, A and B). In addition, Piezo2^{HoxB8} mice remained unresponsive to a brush stroke up to 21 days after nerve injury (Fig. 4D and fig. S9C). These results suggest that nerve injury–induced punctate and dynamic allodynia is Piezo2 dependent.

Another common symptom that manifests in humans with nerve injury–induced pain is hyperalgesia, heightened response to a noxious stimulus (*36*). Because Piezo2^{HoxB8} mice had diminished acute pinprick responses, we tested whether Piezo2 played a role in nerve injury–induced pinprick hyperalgesia. We observed reduced hyperalgesia in Piezo2^{HoxB8} mice 1 week, but not 2 and 3 weeks, after nerve injury (Fig. 4E and fig. S9D). Furthermore, consistent with

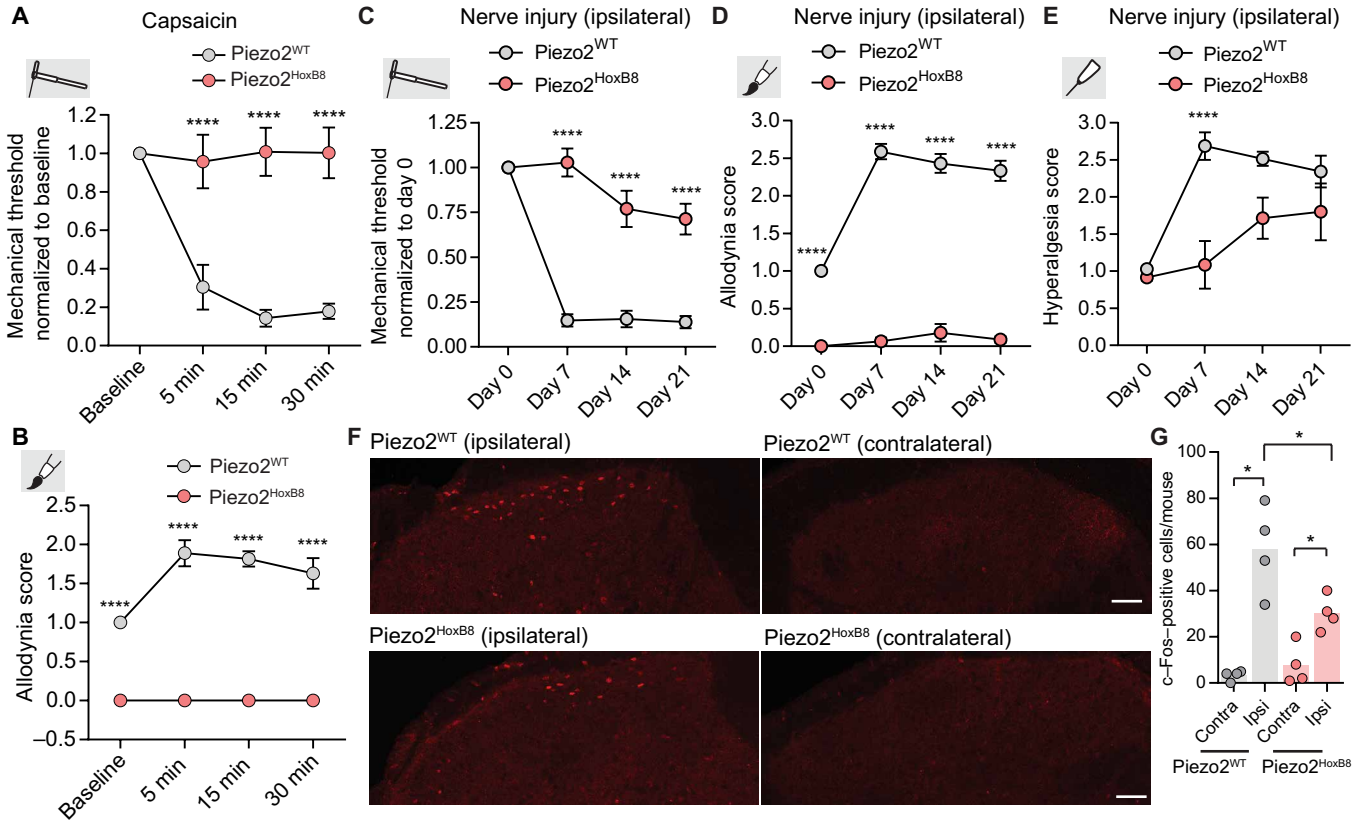

Fig. 4. Capsaicin- and nerve injury–induced mechanical allodynia is mediated by Piezo2. (**A**) Mechanical threshold at baseline (before capsaicin injection) and at 5, 15, and 30 min after capsaicin injection in Piezo2^{WT} ($n = 9$) and Piezo2^{HoxB8} ($n = 9$) mice. (**B**) Dynamic allodynia score measured in response to a paintbrush stroke on the hindpaw before (baseline) and 5, 15, and 30 min after capsaicin injection in Piezo2^{WT} ($n = 9$) and Piezo2^{HoxB8} ($n = 9$) mice. (**C**) Mechanical threshold (Piezo2^{WT}, $n = 13$; Piezo2^{HoxB8}, $n = 13$), (**D**) dynamic allodynia (Piezo2^{WT}, $n = 17$; Piezo2^{HoxB8}, $n = 15$), and (**E**) pinprick hyperalgesia (Piezo2^{WT}, $n = 7$; Piezo2^{HoxB8}, $n = 7$) assessed in Piezo2^{WT} and Piezo2^{HoxB8} mice on days 0 (before injury), 7, 14, and 21 after performing SNI. In (B), (D), and (E), higher score (see Materials and Methods for scoring details) indicates nocifensive behavior. (A to E) ****$P < 0.0001$, two-way ANOVA with Holm-Sidak's multiple comparison test. (**F**) Representative images of pinprick-induced c-Fos immunostaining in dorsal horn of spinal cord of Piezo2^{WT} and Piezo2^{HoxB8} mice on day 21 after SNI, ipsilateral (left) and contralateral (right) to the injury. Scale bars, 50 μm. (**G**) Quantification of number of c-Fos–positive cells in lamina I of the spinal cord (Piezo2^{WT} ipsilateral versus Piezo2^{HoxB8} ipsilateral, *$P = 0.0202$, one-way ANOVA with Tukey's multiple comparison test; Piezo2^{WT}: ipsilateral versus contralateral, *$P = 0.028$; Piezo2^{HoxB8}: ipsilateral versus contralateral, *$P = 0.026$, Mann-Whitney nonparametric analysis).

the behavioral phenotype, we observed reduced pinprick-induced c-Fos expression, a marker of neuronal activity, in the dorsal horn of the spinal cord of Piezo2^{HoxB8} mice compared to wild-type mice (Fig. 4, F and G). This reduction is yet another validation that the attenuated nociceptive behavioral responses are not due to compromised proprioception in these mice. These results suggest that Piezo2 partially mediates nerve injury–induced mechanical hyperalgesia. Because mechanical stimulation–induced sustained firing in Piezo2^{HoxB8} mice is compromised in Aδ-fibers, but not C-fibers, our results suggest that Aδ-fibers could also be implicated in mechanical allodynia (*37*).

DISCUSSION

The results described in this study suggest that Piezo2 is required for mechanical allodynia in mice, whereas noxious mechanosensation is only partially dependent on this ion channel. We find that the approach used to genetically knock out *Piezo2* is critical. While partial or incomplete knockdown of *Piezo2* is sufficient to cause a deficit in touch sensation (*14*, *32*) [see accompanying paper by Szczot *et al.* (*38*)], impaired nociception is apparent only in more complete *Piezo2* knockouts such as the Piezo2^{HoxB8} mice. Although *Piezo2* mRNA is knocked down in 85 to 95% of DRG neurons in Piezo2^{iAdv} mice, it is possible that turnover of Piezo2 protein is too slow to be eliminated entirely from the periphery, which could explain the lack of acute mechanical pain phenotype (*14*) and the remaining capsaicin-induced mechanical allodynia in Piezo2^{iAdv} mice. Because the requirement of Piezo2 in nociception even in Piezo2^{HoxB8} mice is partial, other mechanically activated ion channels that mediate acute mechanical pain sensation must be present. We provide multiple lines of evidence, which argue that the behavioral deficits we observed are not due to proprioceptive defects in Piezo2^{HoxB8} mice: We observe normal behavioral responses to heat; attenuated firing in nociceptors in response to mechanical stimuli; capsaicin-induced thermal hyperalgesia is unaffected; and pinprick-induced c-Fos expression, which is a marker for neuronal activity, is reduced.

How does the same mechanically activated ion channel mediate mechanical allodynia and nociception? We speculate that Piezo2 mediates mechanical allodynia and nociception through its expression in LTMRs and nociceptors, respectively. Piezo2 is highly enriched in LTMRs, and this could explain why touch sensation and allodynia strongly depend on Piezo2 expression (*39*). The Piezo2 modulator stomatin-like 3 protein also plays a direct role in allodynia after nerve injury (*40*), a finding that is consistent with the results reported here. In contrast, the relatively more modest role shown here for Piezo2 in acute nociception and mechanical hyperalgesia could be due to low expression of Piezo2 in nociceptors. Future studies involving selective deletion of Piezo2 in LTMRs or nociceptor subpopulations will elucidate the mechanistic details of how Piezo2 mediates mechanical allodynia.

Consistent with a minor role for Piezo2 in mechanical nociception, Szczot *et al.* (*38*) in this issue report that in individuals with loss-of-function PIEZO2, the threshold to detect pinching of hairy skin is higher; however, due to a small sample size of four patients, a definitive conclusion cannot be made. In contrast to acute nociception, capsaicin-induced mechanical allodynia appears completely dependent on the presence of Piezo2. Finally, our results also show that mechanical allodynia from nerve injury also depends on Piezo2 in mice. Therefore, this raises the possibility that Piezo2 could be a viable clinical target, and Piezo2 blockers might also be efficacious in treating patients suffering from this common cause of mechanical allodynia. Given the widespread and essential role of Piezo2 in touch sensation and proprioception, a systemic inhibition of Piezo2 in the clinic is not practical. Any clinical application would be via topical applications.

There are some limitations of this study that are worth discussing. In the experiments involving optogenetic stimulation of *Piezo2*-expressing neurons, although the weaker response in constitutive Piezo2-ChR2^{+} mice is likely due to incomplete recombination of the viral approach, we cannot exclude the possibility that Piezo2 is more widely expressed in nociceptors during embryonic stages. Whereas we speculate that the lack of acute mechanical pain phenotype in Piezo2^{iAdv} is due to remaining Piezo2 protein at the periphery, immunofluorescent studies with reliable antibodies against Piezo2 will confirm this hypothesis. There is also a possibility that Piezo2 plays an additional unexplored role in sensory processing in the spinal cord and could also contribute to the mechanosensory deficits observed in the Piezo2^{HoxB8} mice. Although this is unlikely because neuronal expression of Piezo2 in the spinal cord has not been observed (*16*), future studies are required to conclusively rule out this possibility.

MATERIALS AND METHODS

Study design

The objective of this study was to determine whether the mechanically activated ion channel Piezo2 plays a role in acute and sensitized mechanical pain sensation. Two genetically different *Piezo2* knockout mouse lines that have been previously characterized by the laboratory were used for the study. Wild-type and *Piezo2* knockout mice were subjected to somatosensory behavioral assays to test responses to innocuous and noxious mechanical stimuli. Impaired responses in *Piezo2* knockout, but not wild-type, mice would be an indication of Piezo2's involvement in mechanosensation. To test Piezo2's contribution to sensitized mechanical pain, we chose an inflammation model that was commonly used in mice and humans, induced by intradermal capsaicin injection. In addition, we also chose a nerve injury model that is widely used in mice to determine nerve injury–mediated sensory sensitization. We supported our behavioral phenotypes with experiments such as optogenetic activation of *Piezo2*-expressing neurons and in vitro and ex vivo electrophysiological recordings. Sample size for behavioral experiments (*15*, *16*, *21*), electrophysiological recordings (*13*, *15*, *21*), and optogenetics experiments (*23*, *41*) were determined on the basis of previous publications and experience from the laboratory. In addition, sample size represents similar number of animals for both sexes. Therefore, data for all behavior and skin-nerve preparation experiments were collected from at least three cohorts of both male and female littermate controls. The experimenter was blinded to genotypes while performing behavior experiments. All animal procedures were approved by the Institutional Animal Care and Use Committees of The Scripps Research Institute (California) and by German federal authorities (state of Berlin).

Animals

Generation of the Advillin-CreERT2 Piezo2 conditional knockout and HoxB8-Cre Piezo2 knockout mice has been previously described

(*14*, *15*). For both Cre lines, Piezo2$^{fl/-}$ mice containing one floxed allele and one null allele were used as Piezo2 knockouts, and littermates that did not carry the Cre allele and were homozygous or heterozygous for the floxed allele were used as controls. CGRP-GFP and MRGPRD-eGFP (*25*) mice were gifts from D. Ginty and M. Zylka, respectively. The Piezo2-GFP-IRES-Cre mouse was generated as previously described (*21*).

Piezo2-GFP-IRES-Cre mice were crossed to Ai32 mice [the Jackson Laboratory (*22*)] that carry the ChR2(H134R)-EYFP construct separated from its CAG promoter by a floxed stop sequence, ensuring the selective expression in Cre-positive tissues. Regarding the viral approach, Piezo2-GFP-IRES-Cre mouse pups (P0 to P2) were intraperitoneally injected with AAV8-CAG-Flex-ChR2-tdtomato virus (10 μl per pup; virus titer, 2×10^{13} genomic copies/ml). Behavioral assessments were conducted at least 4 weeks after injection.

Tamoxifen injections

Tamoxifen was administered as previously described (*14*). Briefly, 15 mg of tamoxifen (Sigma) was dissolved in 1 ml of 100% corn oil and injected intraperitoneally into mice at 150 mg kg^{-1} for five consecutive days. Control and test mice received tamoxifen injections. Behavioral tests were performed between 7 and 14 days after tamoxifen injection. Tamoxifen induction efficiency in Piezo2^{iAdv} was measured by testing tape on back on mice on day 7. Only those mice that showed at least 80% deficit in response were used for further behavioral studies.

Temperature assay

Thermal paw withdrawal threshold was measured as previously described (*42*). Mice were acclimated for 5 min in the provided measurement containers. A thermal probe (which applies about 1*g* of force) (MouseMet Thermal, Topcat Metrology Ltd.) is placed against the plantar surface of the mouse paw. Before coming into contact with the paw, the probe is preheated to ~37°C. After contact, the probe heats at a rate of 2.5°C/s, and paw removal from the probe triggers the display of the withdrawal temperature on the readout. Note that to prevent tissue injury, the probe automatically shuts off at 60°C. The average of three attempts recorded per mouse is reported.

Innocuous touch assays

Mechanical threshold

Mice were acclimated for 1 hour in von Frey chambers. Fifty percent mechanical threshold was measured with calibrated von Frey filaments (0.07*g*, 0.16*g*, 0.4*g*, 0.6*g*, 1.0*g*, 1.4*g*, 2.0*g*, 4.0*g*, and 6.0*g*) using the up-down method (*26*). Values were normalized to baseline in Fig. 4, because there were large differences in absolute mechanical threshold values between Piezo2^{WT} and Piezo2^{HoxB8} mice.

Tape response assay

Mice were acclimated in a round plexiglass container for at least 5 min. A 1-inch piece of laboratory tape was placed gently on the bottom center of the mouse's back. Mice were observed for a duration of 5 min, and the total number of bouts in response to the tape was recorded and reported. Biting or scratching of the tape or a visible "wet dog shake" motion to remove the tape on its back was scored as a response.

Cotton swab assay

Response to a gentle stroke was assessed by stroking a cotton swab on the plantar surface of the hindpaw, as described previously (*14*). Mice were acclimated for 1 hour in von Frey chambers. A cotton swab from a Q-tip was manually pulled such that it was puffed out to three times its size. A paw withdrawal motion in response to a stroke of the swab underneath the mouse paw was scored. Five sweeps were performed with at least 10 s between each. The number of withdrawals out of five trials was counted and reported as percentage withdrawal for each mouse.

Single force von Frey hairs

Mice were acclimated in von Frey chambers for 1 hour. Von Frey hairs at forces of 4*g*, 2*g*, 1.4*g*, 1*g*, 0.6*g*, 0.4*g*, 0.16*g*, 0.07*g*, 0.04*g*, 0.02*g*, and 0.008*g* were applied directly underneath the glabrous skin of the hindpaw until the hairs bent slightly, and a response within the next 1 s was recorded. Each filament was applied four times, and the total number of responses per force was reported as percentage withdrawal per mouse.

Dynamic allodynia

Dynamic allodynia was measured before and after capsaicin injection or SNI, as described previously (*43*). Mice were acclimated in von Frey chambers for 1 hour. A 5/0 brush was gently stroked on the lateral side of the hindpaw from heel to toe. The response was scored as follows: 0 = no response; 1 = very short, fast movement/lifting of the paw; 2 = sustained lifting of the paw for more than 2 s toward the body or strong lateral lifting above the body level; and 3 = flinching, licking, or flicking of the affected paw. Average scores across three trials per mouse were reported as an allodynia score. For SNI experiments, baseline was measured only on the ipsilateral paw.

Blink reflex assay

While the mouse was scruffed, the peripheral cornea of the right eye was gently touched with a von Frey filament (0.008*g*, 0.04*g*, or 0.4*g*) until the filament bent slightly. One force was tested per day, and each filament was applied five times with a 5-s interval between stimuli. Two observers reported positive or negative blink responses, and only when both reported positively was it considered a reflexive blink.

Pain assays

Response to pinprick

Mice were acclimated in von Frey chambers for 1 hour. A 27-gauge needle was applied to the glabrous skin of the hindpaw, taking care not to pierce through the skin. Ten trials per mouse were performed with 1-min intervals between each trial. Paw withdrawal, shaking, or licking was scored as a response and reported as percentage for the total number of trials. A new needle was used for each mouse. In the Piezo2^{HoxB8} mice, a no response was called when mice failed to respond within 20 s.

Pinprick hyperalgesia

To assess hypersensitivity to pinprick response after SNI, the response to pinprick was scored as follows: 0 = no movement, 1 = short lift, 2 = sustained lift, and 3 = flinching or licking of affected paw. The average score across five trials per mouse was reported as a hyperalgesia score. Baseline was measured only for the ipsilateral side.

Tail clip

Response to blunt pressure application was assessed with the tail clip assay, as previously mentioned (*14*). Briefly, mice were first acclimated for 5 min in round plexiglass containers. A calibrated alligator clip (500*g*) was applied to the middle of the tail, and the mouse was placed back into the plexiglass container. A response was scored when the mice showed awareness of the clip by biting, vocalization, grasping of the tail, or a jumping response. A cutoff of 120 s was

applied to prevent tissue damage. Time to respond was recorded and reported as latency for each mouse.

SNI model

The SNI model was adapted from (*44*). All surgeries were performed on adult mice (10 to 12 weeks) that were anesthetized with isoflurane (0.5 to 3.0%). After first exposing the sciatic nerve in the thigh region of the adult mouse, the tibial and common peroneal nerves were ligated with a 5-0 silk suture and then cut into two places, with the piece of nerve between the cuts being removed. The sural nerve was left intact. Mechanical threshold, dynamic allodynia, and pinprick hyperalgesia were tested on day 0 (baseline: before performing surgery) and on days 7, 14, and 21 after surgery. Mechanical stimulation was applied to the lateral region of the injured paw, where the sural nerve specifically enervates.

Capsaicin-mediated hypersensitivity

Capsaicin (10 μl) [0.1 g ml^{-1} 100% ethanol, 1:1000 phosphate-buffered saline (PBS), 0.5% Tween 80, 10% ethanol] or vehicle (1:1000 PBS, 0.5% Tween 80, 10% ethanol) was administered via intraplantar injections. Paw size was measured before and after 10 min of capsaicin injection using the digimatic thickness gage (Mitutoyo Corporation, no. 99MAG011M, series no. 547, 7300). Mechanical stimulation was performed before injecting (baseline) and 5, 15, and 30 min after injecting the indicated compound.

Thermal hyperalgesia

Mice were habituated to scruffing for 4 days before testing. Latency to response was measured as the time from when the paw was submerged in a water bath at 45°C until a response. Responses such as paw withdrawal, guarding, and vocalization were scored as a positive response. A 30-s cutoff was enforced to avoid discomfort or pain to the mice. Three measurements were taken per mouse, and an average value per mouse was reported.

Acute light-evoked pain responses

Acute nocifensive behaviors in Piezo2-$ChR2^+$ mice were evaluated as described previously (*23*). Briefly, mice were habituated for 1 hour before any optical stimulation. A 462-nm blue diode laser or a 589-nm diode-pumped solid-state yellow laser (Shanghai Lasers & Optics Century) was coupled to an optic fiber (1 mm diameter, Prizmatix) to aim and deliver light to the plantar surface of the hindpaw. Yellow light was used as a control stimulus that does not activate ChR2. Each trial consisted of a 20-s optical stimulation (2-Hz pulsing frequency, 100-ms pulse duration) set at different light intensities (0.151 to 2.14 mW/mm^2). For each intensity, a total of two to four trials per animal were performed alternating between the left and right hindpaws. Scored nocifensive behaviors included hindpaw withdrawal, licking, guarding, flinching, jumping, and audible vocalization. The percentage of trials during which these behaviors occurred is quantified. Photostimulation with yellow light did not evoke any behavioral response ($n = 8$).

DRG culture and siRNA

Mouse DRG neurons were isolated and cultured with the procedure as described (*13*). For Piezo2 knockdown experiments, freshly isolated DRG neurons were nucleofected with scrambled or 250 nM *Piezo2* siRNA [SMARTpool: ON-TARGETplus *Piezo2* siRNA, Dharmacon L-163012-00-0005, previously validated in (*13*)] along with tdTomato (200 ng). After nucleofection (4D-Nucleofector System, Lonza), neurons were allowed to recover in RPMI medium for 10 min at 37°C, growth medium [with antibiotics and without cytosine arabinoside (AraC)] was added, and neurons were plated on laminin (2 μg ml^{-1})–coated poly-D-lysine coverslips. Growth medium supplemented with growth factors was added an hour after plating. Knockdown efficiency was measured by quantitative real-time polymerase chain reaction (PCR) against *Piezo2*. Eighty percent and eighty two percent knockdown of Piezo2 were achieved in MRGPRD-GFP DRG neurons from two independent experiments. Mechanically activated currents were recorded on days 3 and 4 after nucleofection and from cells that were tdTomato and strongly GFP positive. Data were combined from two experimenters across two to three independent experiments.

Quantitative real-time PCR analysis

Quantitative PCR (qPCR) analysis was performed as previously described (*14*). Briefly, total RNA was extracted using TRIzol/chloroform and isopropanol precipitation from freshly isolated DRG neurons (Life Technologies). Generation of complementary DNA (cDNA) was achieved by reverse transcription using the QuantiTect Reverse Transcript Kit (Qiagen). For qPCR, FastStart Universal probe master mix (Rox) from Roche Diagnostics was used. The reaction was run in the Eco Real-Time PCR instrument (Illumina) using 0.5 μl of the cDNA in a 10-μl reaction according to the manufacturer's instructions. Real-time TaqMan qPCR assays were purchased from Integrated DNA Technologies with a FAM reporter dye and a nonfluorescent quencher: mouse *Piezo2* (Mm.PT.56a.32860700) and an internally designed mouse *Gapdh* assay (forward primer, 5′-GCACCACCAACTGCTTAG-′3; reverse primer, 5′-GGATGCAGGGATGATGTTC-′3; and probe, 5′-CAGAAGACTGTGGATGGCCCCTC-′3).

Electrophysiology and mechanical stimulation

Mechanically activated currents from DRG neurons were recorded in whole-cell patch clamp mode using either an Axopatch 200B or MultiClamp700A amplifier. Currents were sampled at 20 kHz and filtered at 2 kHz. Recording electrodes had a resistance of 4 to 7 megohms when filled with gluconate-based low-chloride intracellular solution: 125 mM K-gluconate, 7 mM KCl, 1 mM $CaCl_2$, 1 mM $MgCl_2$, 10 mM Hepes (pH with KOH), 1 mM tetra-K BAPTA [1,2-bis(2-aminophenoxy)ethane-*N*,*N*,*N*′,*N*′-tetraacetic acid], 4 mM Mg-ATP (adenosine triphosphate), and 0.5 Na-GTP (guanosine triphosphate). Extracellular bath solution was composed of 133 mM NaCl, 3 mM KCl, 2.5 mM $CaCl_2$, 1 mM $MgCl_2$, 10 mM Hepes (pH 7.3 with NaOH), and 10 mM glucose.

Mechanical stimulation was achieved using a fire-polished glass pipette (tip diameter, 3 to 4 μm) positioned at an angle of 80° relative to the cell being recorded. Displacement of the probe toward the cell was driven by Clampex-controlled piezoelectric crystal microstage (E625 LVPZT Controller/Amplifier; Physik Instrumente). The probe had a velocity of 1 μm ms^{-1} during the ramp phase of the command for forward movement, and the stimulus was applied for a duration of 150 ms. For each cell, a series of mechanical steps in 0.5- or 1-μm increments was applied every 10 or 30 s.

c-Fos induction and immunostaining

Pinprick-induced c-Fos expression was induced by gently pricking the plantar surface of the hindpaw of a mouse repeatedly for 15 min in 2-s intervals. Mice were lightly anesthetized with isoflurane during the stimulation period. One hour from the midway of the stimulation period, mice were intracardially perfused with PBS followed by 4% paraformaldehyde (PFA). The spinal cord was then

isolated and post-fixed with 4% PFA for 1 hour at 4°C. PFA (4%) was replaced with 30% sucrose, and the tissue was incubated overnight at 4°C and finally sectioned at a thickness of 25 μm for c-Fos immunostaining.

Sections were first washed two times for 15 min in PBS to remove excess optimal cutting temperature (OCT) compound. They were then incubated in blocking serum [10% normal goat serum (NGS) in PBS with 0.1% Triton X-100 (PBS-T)] for 1 hour at room temperature. Sections were then rinsed three times in 0.1% PBS-T for 15 min. After rinsing, they were incubated with rabbit anti–c-Fos polyclonal antibody (diluted 1:500 in 0.1% PBS-T with 1% NGS; Millipore, catalog no. ABE-457) and mouse anti-CGRP polyclonal antibody (diluted 1:500 in 0.1% PBS-T with 1% NGS; Abcam, catalog no. ab81887) overnight at 4°C. The following day, the sections were washed three times for 15 min in 0.1% PBS-T and then incubated in secondary antibody (biotinylated goat anti-rabbit IgG Alexa 594, 1:500; Invitrogen, A11307; biotinylated goat anti-mouse IgG Alexa 488, 1:500; Invitrogen, A21121) for 2 hours at room temperature covered in aluminum foil. Sections were then washed three times for 15 min in 0.1% PBS-T, mounted with DAPI Fluoromount-G (SouthernBiotech, catalog no. 0100-20), and imaged.

Images were taken on a Nikon A1 inverted laser scanning confocal microscope at 10× and 20× and analyzed with Nikon NIS Elements Software. c-Fos–positive neurons were counted only in lamina I of the spinal cord using CGRP staining to draw regions of interest on the ipsilateral and contralateral side. c-Fos–positive neurons were added from three lumbar spinal cord sections for each mouse and reported as an average across four mice for wild-type and Piezo2^{HoxB8} genotypes.

Skin-nerve preparation experiments

Sensory neuron recordings with skin-nerve preparation were performed in accordance with previously published procedures (*45*, *46*). Mice were euthanized by CO_2 inhalation for 2 to 4 min followed by cervical dislocation. The saphenous nerve and shaved hairy skin of the hindlimb were dissected free and placed in an organ bath of 32°C perfused with a synthetic interstitial fluid buffer: 123 mM NaCl, 3.5 mM KCl, 0.7 mM $MgSO_4$, 1.7 mM NaH_2PO_4, 2.0 mM $CaCl_2$, 9.5 mM sodium gluconate, 5.5 mM glucose, 7.5 mM sucrose, and 10 mM Hepes (pH 7.4). The saphenous nerve was placed in an adjacent chamber in mineral oil, where fine filaments were teased from the nerve and placed on the recording electrode.

In electrical search experiments, a microelectrode (0.5 to 1 megohms) was placed in contact with the epineurium of the saphenous nerve and electrical stimulations were given at a rate of 1 Hz with intervals of spare pulses of 50- to 500-ms duration. Nerve stimulation was performed at nerve branch points to trace individual fibers to their receptive fields. On the basis of conduction velocity, units were categorized as Aβ-, Aδ-, and C-fibers. Mechanical probing of the electrical receptive field was then performed to test for mechanical sensitivity.

In separate experiments, mechanically sensitive units were characterized by conduction velocity, and stimulus response functions were obtained. Single-unit receptive fields were stimulated with a mechanical stimulating probe equipped with a computer-controlled force measurement system (nanomotor, Kleindiek). The probe was a stainless steel metal rod with a contact area diameter of 0.8 mm. Slowly adapting Aβ-, Aδ-, and C-fibers were stimulated with five ramp and hold stimuli of increasing amplitudes (from 20 to 400 mN) at 30- to 60-s intervals. Mechanical thresholds were measured by reading the force that elicited the first spike. Aβ-fibers and low-threshold Aδ-fibers (D hairs) were stimulated with a piezo actuator (Physik Instrumente) using a protocol with increasing ramp velocities (0.075, 0.15, 0.45, and 1.5 mm s^{-1}). In a subset of experiments, thermal-evoked firing activity of thermoreceptive C fibers was also recorded. A computer-controlled thermal Peltier stimulator with a stimulating area diameter of 5 mm^2 was used to apply thermal stimuli (custom device built by Yale School of Medicine Instrumentation Repair and Design). Two heat stimuli were used: a 4-s ramp and hold stimulus from 32° to 48°C, and a continuous heat ramp from 32° to 48°C at a rate of 1°C/s. Experimenters were blinded to mouse genotype in all experiments.

In situ hybridization

In situ hybridization was performed on fresh-frozen lumbar DRG sections using RNAscope technology according to the manufacturer's instructions (ACDBio; Kit #323110, Piezo2 probe #439971). Images were acquired using a Nikon C2 laser scanning confocal microscope (20×; numerical aperture, 0.9) at matched camera settings for each staining experiment. Piezo2 transcript labeling was quantified using Nikon Elements software. Regions of interest were drawn around all DRG cell bodies (excluding nerve tracts) using DAPI fluorescence as a guide (n = 7 to 17 sections per animal). To avoid background, pixels in the lowest 10% of intensity values were excluded via thresholding, and remaining pixel area and pixel intensity values were recorded within the regions of interest. Area of transcript labeling was quantified as a fraction of total regions of interest area. Mean values for all sections per animal were calculated and then represented as a percent of the brightest wild-type values from the parallel staining experiment.

Statistical analysis

Statistical significance was computed using GraphPad Prism 6. Mann-Whitney tests were performed when comparison was made between two groups. One-way and two-way ANOVA with multiple comparison tests were performed when data between two groups, at multiple time points, were compared. In Fig. 3B, the bar graph is a quantification of number of fibers that respond to mechanical poking or not, and statistically cannot be determined whether one group is significantly different from the other. A χ^2 analysis was performed to determine trend (χ^2 = 3.13, 1; P = 0.077). When Bonferroni correction has been made, it has been stated in the figure legend. Sample size, P value (α = 0.05, two sided), and statistical tests used are indicated in figure legends.

SUPPLEMENTARY MATERIALS

www.sciencetranslationalmedicine.org/cgi/content/full/10/462/eaat9897/DC1

Fig. S1. Genetic strategy to generate Piezo2-ChR2 mice.

Fig. S2. Mechanically activated currents in nociceptor subtypes of DRG neurons are Piezo2 dependent.

Fig. S3. Response to mechanosensory stimulation of the eye (the blink reflex) is normal in Piezo2^{HoxB8} mice.

Fig. S4. Response to innocuous and noxious stimuli in Piezo2^{HoxB8} mice is not dependent on the sex of the animal.

Fig. S5. Aδ- and C-fiber mechanical and thermal thresholds in Piezo2^{HoxB8} mice.

Fig. S6. Capsaicin-induced thermal hyperalgesia is unaffected in Piezo2^{HoxB8} mice.

Fig. S7. Capsaicin-induced mechanical sensitization in Piezo2^{WT} and Piezo2^{HoxB8} mice.

Fig. S8. Capsaicin-induced mechanical allodynia is compromised in Piezo2^{iAdv} mice.

Fig. S9. SNI-induced mechanical sensitization in Piezo2^{WT} and Piezo2^{HoxB8} mice.

Table S1. Source data for Figs. 1, 2, and 4 and figs. S1, S3, S5, S6, and S8.

REFERENCES AND NOTES

1. M. Costigan, J. Scholz, C. J. Woolf, Neuropathic pain: A maladaptive response of the nervous system to damage. *Annu. Rev. Neurosci.* **32**, 1–32 (2009).
2. C. J. Woolf, Central sensitization: Implications for the diagnosis and treatment of pain. *Pain* **152**, S2–S15 (2011).
3. J. N. Campbell, R. A. Meyer, Mechanisms of neuropathic pain. *Neuron* **52**, 77–92 (2006).
4. A. Truini, L. Garcia-Larrea, G. Cruccu, Reappraising neuropathic pain in humans—How symptoms help disclose mechanisms. *Nat. Rev. Neurol.* **9**, 572–582 (2013).
5. M. Koltzenburg, L. E. Lundberg, H. E. Torebjörk, Dynamic and static components of mechanical hyperalgesia in human hairy skin. *Pain* **51**, 207–219 (1992).
6. J. L. Ochoa, D. Yarnitsky, Mechanical hyperalgesias in neuropathic pain patients: Dynamic and static subtypes. *Ann. Neurol.* **33**, 465–472 (1993).
7. P. J. Austin, G. Moalem-Taylor, Animal models of neuropathic pain due to nerve injury, in *Stimulation and Inhibition of Neurons*, P. M. Pilowsky, M. M. Farnham, A. Y. Fong, Eds. (Springer, 2012), vol. 78, pp. 239–260.
8. A. S. Jaggi, V. Jain, N. Singh, Animal models of neuropathic pain. *Fundam. Clin. Pharmacol.* **25**, 1–28 (2011).
9. M. Colleoni, P. Sacerdote, Murine models of human neuropathic pain. *Biochim. Biophys. Acta* **1802**, 924–933 (2010).
10. V. E. Abraira, D. D. Ginty, The sensory neurons of touch. *Neuron* **79**, 618–639 (2013).
11. C. J. Woolf, Q. Ma, Nociceptors—Noxious stimulus detectors. *Neuron* **55**, 353–364 (2007).
12. A. I. Basbaum, D. M. Bautista, G. Scherrer, D. Julius, Cellular and molecular mechanisms of pain. *Cell* **139**, 267–284 (2009).
13. B. Coste, J. Mathur, M. Schmidt, T. J. Earley, S. Ranade, M. J. Petrus, A. E. Dubin, A. Patapoutian, Piezo1 and Piezo2 are essential components of distinct mechanically activated cation channels. *Science* **330**, 55–60 (2010).
14. S. S. Ranade, S.-H. Woo, A. E. Dubin, R. A. Moshourab, C. Wetzel, M. Petrus, J. Mathur, V. Bégay, B. Coste, J. Mainquist, A. J. Wilson, A. G. Francisco, K. Reddy, Z. Qiu, J. N. Wood, G. R. Lewin, A. Patapoutian, Piezo2 is the major transducer of mechanical forces for touch sensation in mice. *Nature* **516**, 121–125 (2014).
15. S.-H. Woo, V. Lukacs, J. C. de Nooij, D. Zaytseva, C. R. Criddle, A. Francisco, T. M. Jessell, K. A. Wilkinson, A. Patapoutian, Piezo2 is the principal mechanotransduction channel for proprioception. *Nat. Neurosci.* **18**, 1756–1762 (2015).
16. K. Nonomura, S.-H. Woo, R. B. Chang, A. Gillich, Z. Qiu, A. G. Francisco, S. S. Ranade, S. D. Liberles, A. Patapoutian, Piezo2 senses airway stretch and mediates lung inflation-induced apnoea. *Nature* **541**, 176–181 (2016).
17. A. T. Chesler, M. Szczot, D. Bharucha-Goebel, M. Čeko, S. Donkervoort, C. Laubacher, L. H. Hayes, K. Alter, C. Zampieri, C. Stanley, A. M. Innes, J. K. Mah, C. M. Grosmann, N. Bradley, D. Nguyen, A. R. Foley, C. E. Le Pichon, C. G. Bönnemann, The role of PIEZO2 in human mechanosensation. *N. Engl. J. Med.* **375**, 1355–1364 (2016).
18. R. Witschi, T. Johansson, G. Morscher, L. Scheurer, J. Deschamps, H. Ulrich Zeilhofer, Hoxb8-Cre mice: A tool for brain-sparing conditional gene deletion. *Genesis* **48**, 596–602 (2010).
19. M. Szczot, L. A. Pogorzala, H. Jürgen Solinski, L. Young, P. Yee, C. E. Le Pichon, A. T. Chesler, M. A. Hoon, Cell-type-specific splicing of Piezo2 regulates mechanotransduction. *Cell Rep.* **21**, 2760–2771 (2017).
20. M. Q. Nguyen, Y. Wu, L. S. Bonilla, L. J. von Buchholtz, N. J. P. Ryba, Diversity amongst trigeminal neurons revealed by high throughput single cell sequencing. *PLOS ONE* **12**, e0185543 (2017).
21. S.-H. Woo, S. Ranade, A. D. Weyer, A. E. Dubin, Y. Baba, Z. Qiu, M. Petrus, T. Miyamoto, K. Reddy, E. A. Lumpkin, C. L. Stucky, A. Patapoutian, Piezo2 is required for Merkel-cell mechanotransduction. *Nature* **509**, 622–626 (2014).
22. L. Madisen, T. Mao, H. Koch, J.-M. Zhuo, A. Berenyi, S. Fujisawa, Y.-W. A. Hsu, A. J. Garcia III, X. Gu, S. Zanella, J. Kidney, H. Gu, Y. Mao, B. M. Hooks, E. S. Boyden, G. Buzsáki, J. Marino Ramirez, A. R. Jones, K. Svoboda, X. Han, E. E. Turner, H. Zeng, A toolbox of Cre-dependent optogenetic transgenic mice for light-induced activation and silencing. *Nat. Neurosci.* **15**, 793–802 (2012).
23. I. Daou, A. H. Tuttle, G. Longo, J. S. Wieskopf, R. P. Bonin, A. R. Ase, J. N. Wood, Y. De Koninck, A. Ribeiro-da-Silva, J. S. Mogil, P. Séguéla, Remote optogenetic activation and sensitization of pain pathways in freely moving mice. *J. Neurosci.* **33**, 18631–18640 (2013).
24. D. J. Cavanaugh, H. Lee, L. Lo, S. D. Shields, M. J. Zylka, A. I. Basbaum, and D. J. Anderson, Distinct subsets of unmyelinated primary sensory fibers mediate behavioral responses to noxious thermal and mechanical stimuli. *Proc. Natl. Acad. Sci. U.S.A.* **106**, 9075–9080 (2009).
25. M. J. Zylka, F. L. Rice, D. J. Anderson, Topographically distinct epidermal nociceptive circuits revealed by axonal tracers targeted to Mrgprd. *Neuron* **45**, 17–25 (2005).
26. S. R. Chaplan, F. W. Bach, J. W. Pogrel, J. M. Chung, T. L. Yaksh, Quantitative assessment of tactile allodynia in the rat paw. *J. Neurosci. Methods* **53**, 55–63 (1994).
27. A. Arcourt, L. Gorham, R. Dhandapani, V. Prato, F. J. Taberner, H. Wende, V. Gangadharan, C. Birchmeier, P. A. Heppenstall, S. G. Lechner, Touch receptor-derived sensory information alleviates acute pain signaling and fine-tunes nociceptive reflex coordination. *Neuron* **93**, 179–193 (2017).
28. C. E. Le Pichon, A. T. Chesler, The functional and anatomical dissection of somatosensory subpopulations using mouse genetics. *Front. Neuroanat.* **8**, 21 (2014).
29. A. E. Dubin, A. Patapoutian, Nociceptors: The sensors of the pain pathway. *J. Clin. Invest.* **120**, 3760–3772 (2010).
30. R. Schmidt, M. Schmelz, H. E. Torebjörk, H. O. Handwerker, Mechano-insensitive nociceptors encode pain evoked by tonic pressure to human skin. *Neuroscience* **98**, 793–800 (2000).
31. M. Koltzenburg, H. O. Handwerker, Differential ability of human cutaneous nociceptors to signal mechanical pain and to produce vasodilatation. *J. Neurosci.* **14**, 1756–1765 (1994).
32. N. Eijkelkamp, J. E. Linley, J. M. Torres, L. Bee, A. H. Dickenson, M. Gringhuis, M. S. Minett, G. S. Hong, E. Lee, U. Oh, Y. Ishikawa, F. J. Zwartkuis, J. J. Cox, J. N. Wood, A role for Piezo2 in EPAC1-dependent mechanical allodynia. *Nat. Commun.* **4**, 1682 (2013).
33. L. F. Ferrari, O. Bogen, P. Green, J. D. Levine, Contribution of Piezo2 to endothelium-dependent pain. *Mol. Pain* **11**, 65 (2015).
34. N. Gregory, A. L. Harris, C. R. Robinson, P. M. Dougherty, P. N. Fuchs, K. A. Sluka, An overview of animal models of pain: Disease models and outcome measures. *J. Pain* **14**, 1255–1269 (2013).
35. M. Tominaga, M. J. Caterina, A. B. Malmberg, T. A. Rosen, H. Gilbert, K. Skinner, B. E. Raumann, A. I. Basbaum, D. Julius, The cloned capsaicin receptor integrates multiple pain-producing stimuli. *Neuron* **21**, 531–543 (1998).
36. R.-D. Treede, R. A. Meyer, S. N. Raja, J. N. Campbell, Peripheral and central mechanisms of cutaneous hyperalgesia. *Prog. Neurobiol.* **38**, 397–421 (1992).
37. R. Dhandapani, C. Mary Arokiaraj, F. J. Taberner, P. Pacifico, S. Raja, L. Nocchi, C. Portulano, F. Franciosa, M. Maffei, A. Fawzi Hussain, F. de Castro Reis, L. Reymond, E. Perlas, S. Garcovich, S. Barth, K. Johnsson, S. G. Lechner, P. A. Heppenstall, Control of mechanical pain hypersensitivity in mice through ligand-targeted photoablation of TrkB-positive sensory neurons. *Nat. Commun.* **9**, 1640 (2018).
38. M. Szczot, J. Liljencrantz, N. Ghitani, A. Barik, R. Lam, J. H. Thompson, D. Bharucha-Goebel, D. Saade, A. Necaise, S. Donkervoort, A. R. Foley, T. Gordon, L. Case, M. C. Bushnell, C. G. Bönnemann, A. T. Chesler, PIEZO2 mediates injury-induced tactile pain in mice and humans. *Sci. Transl. Med.* **10**, eaat9892 (2018).
39. D. Usoskin, A. Furlan, S. Islam, H. Abdo, P. Lönnerberg, D. Lou, J. Hjerling-Leffler, J. Haeggström, O. Kharchenko, P. V. Kharchenko, S. Linnarsson, P. Ernfors, Unbiased classification of sensory neuron types by large-scale single-cell RNA sequencing. *Nat. Neurosci.* **18**, 145–153 (2014).
40. C. Wetzel, S. Pifferi, C. Picci, C. Gök, D. Hoffmann, K. K. Bali, A. Lampe, L. Lapatsina, R. Fleischer, E. St John Smith, V. Bégay, M. Moroni, L. Estebanez, J. Kühnemund, J. Walcher, E. Specker, M. Neuenschwander, J. P. von Kries, V. Haucke, R. Kuner, J. F. A. Poulet, J. Schmoranzer, K. Poole, G. R. Lewin, Small-molecule inhibition of STOML3 oligomerization reverses pathological mechanical hypersensitivity. *Nat. Neurosci.* **20**, 209–218 (2016).
41. I. Daou, H. Beaudry, A. R. Ase, J. S. Wieskopf, A. Ribeiro-da-Silva, J. S. Mogil, P. Séguéla, Optogenetic silencing of $Na_V1.8$-positive afferents alleviates inflammatory and neuropathic pain. *eNeuro* **3**, ENEURO.0140-0115.2016 (2016).
42. J. R. Deuis, I. Vetter, The thermal probe test: A novel behavioral assay to quantify thermal paw withdrawal thresholds in mice. *Temperature* **3**, 199–207 (2016).
43. B. Duan, L. Cheng, S. Bourane, O. Britz, C. Padilla, L. Garcia-Campmany, M. Krashes, W. Knowlton, T. Velasquez, X. Ren, S. Ross, B. B. Lowell, Y. Wang, M. Goulding, Q. Ma, Identification of spinal circuits transmitting and gating mechanical pain. *Cell* **159**, 1417–1432 (2014).
44. A.-F. Bourquin, M. Süveges, M. Pertin, N. Gilliard, S. Sardy, A. C. Davison, D. R. Spahn, I. Decosterd, Assessment and analysis of mechanical allodynia-like behavior induced by spared nerve injury (SNI) in the mouse. *Pain* **122**, 14.e11–14.e14 (2006).
45. C. Wetzel, J. Hu, D. Riethmacher, A. Benckendorff, L. Harder, A. Eilers, R. Moshourab, A. Kozlenkov, D. Labuz, O. Caspani, B. Erdmann, H. Machelska, P. A. Heppenstall, G. R. Lewin, A stomatin-domain protein essential for touch sensation in the mouse. *Nature* **445**, 206–209 (2006).
46. M. Koltzenburg, C. L. Stucky, G. R. Lewin, Receptive properties of mouse sensory neurons innervating hairy skin. *J. Neurophysiol.* **78**, 1841–1850 (1997).

Acknowledgments: We thank K. Spencer for help with imaging; A. Coombs for technical support; G. Gatto and S. C. Koch for help with c-Fos staining; V. Bégay and M. Braunschweig for assistance with mice; and A. Moqrich, Q. Ma, S. Ranade, and M. Petrus for helpful discussions on behavior. **Funding:** This work was supported by NIH grants R01 DE022358 and R35

NS105067 to A.P., who is also an investigator of the Howard Hughes Medical Institute. Additional support was provided from an ERC grant (AdG 789128) to G.R.L. J.K. was supported by stipend from the Berlin Institute for Health (BIH). I.D. is funded by a postdoctoral fellowship from Canadian Institutes of Health Research. A.E.D. is funded by the NIH (R21DE025329). **Author contributions:** A.P. and S.E.M. designed experiments. M.C.L., S.E.M., and A.G.F. performed and analyzed behavioral experiments. S.E.M. and W.T.K. performed the blink reflex assay. I.D. performed optogenetic experiments. F.S. and J.K. performed and analyzed ex vivo skin-nerve preparation experiments with input from G.R.L. K.L.M. performed RNA scope experiments. S.E.M. and A.E.D. performed and analyzed in vitro electrophysiological experiments. S.E.M. and A.P. wrote the manuscript with input from all authors. **Competing interests:** The authors declare that they have no competing interests. **Data and materials availability:** All the data are in the main text or in the Supplementary Materials.

Submitted 25 April 2018
Accepted 19 September 2018
Published 10 October 2018
10.1126/scitranslmed.aat9897

Citation: S. E. Murthy, M. C. Loud, I. Daou, K. L. Marshall, F. Schwaller, J. Kühnemund, A. G. Francisco, W. T. Keenan, A. E. Dubin, G. R. Lewin, A. Patapoutian, The mechanosensitive ion channel Piezo2 mediates sensitivity to mechanical pain in mice. *Sci. Transl. Med.* **10**, eaat9897 (2018).

Science Translational Medicine

The mechanosensitive ion channel Piezo2 mediates sensitivity to mechanical pain in mice

Swetha E. Murthy, Meaghan C. Loud, Ihab Daou, Kara L. Marshall, Frederick Schwaller, Johannes Kühnemund, Allain G. Francisco, William T. Keenan, Adrienne E. Dubin, Gary R. Lewin and Ardem Patapoutian

Sci Transl Med **10**, eaat9897.
DOI: 10.1126/scitranslmed.aat9897

Understanding pain sensitization

Inflammation or nerve injury can alter tactile sensation, making a gentle touch perceived as painful. The molecular mechanisms mediating this alteration in sensation, called mechanical allodynia, are not completely understood. Murthy *et al*. and Szczot *et al*. discovered that PIEZO2 ion channels expressed in sensory neurons are required for the development of mechanical allodynia in mice and humans. The authors independently reached this conclusion using different animal models. Szczot *et al*. extended the discovery to humans, showing that PIEZO2 loss of function resulted in failure to develop mechanical allodynia. These two studies suggest that local inhibition of PIEZO2 ion channels might be effective for treating mechanical allodynia.